AGU PUBLICATIONS

JGR

Journal of Geophysical Research: Atmospheres

RESEARCH ARTICLE

10.1002/2017JD027562

Key Points:
- Greenhouse gas increases and stratospheric ozone depletion contribute nearly equally to the simulated mean age decrease in 1960–2010
- Stratospheric ozone depletion causes an increase in mean age in the Antarctic summer lower stratosphere
- The relative impacts of greenhouse gases and stratospheric ozone on trends of mean age and the residual circulations are different

Correspondence to:
F. Li,
feng.li@nasa.gov

Citation:
Li, F., Newman, P., Pawson, S., & Perlwitz, J. (2018). Effects of greenhouse gas increase and stratospheric ozone depletion on stratospheric mean age of air in 1960–2010. *Journal of Geophysical Research: Atmospheres*, *123*, 2098–2110. https://doi.org/10.1002/2017JD027562

Received 4 AUG 2017
Accepted 4 FEB 2018
Accepted article online 10 FEB 2018
Published online 23 FEB 2018

Effects of Greenhouse Gas Increase and Stratospheric Ozone Depletion on Stratospheric Mean Age of Air in 1960–2010

Feng Li[1,2], **Paul Newman**[2], **Steven Pawson**[2], **and Judith Perlwitz**[3,4]

[1]Universities Space Research Association, Columbia, MD, USA, [2]NASA Goddard Space Flight Center, Greenbelt, MD, USA, [3]Cooperative Institute for Research in Environmental Sciences, University of Colorado, Boulder, CO, USA, [4]Physical Sciences Division, NOAA Earth System Research Laboratory, Boulder, CO, USA

Abstract The relative impacts of greenhouse gas (GHG) increase and stratospheric ozone depletion on stratospheric mean age of air in the 1960–2010 period are quantified using the Goddard Earth Observing System Chemistry-Climate Model. The experiment compares controlled simulations using a coupled atmosphere-ocean version of the Goddard Earth Observing System Chemistry-Climate Model, in which either GHGs or ozone depleting substances, or both factors evolve over time. The model results show that GHGs and ozone depleting substances have about equal contributions to the simulated mean age decrease, but GHG increases account for about two thirds of the enhanced strength of the lower stratospheric residual circulation. It is also found that both the acceleration of the diabatic circulation and the decrease of the mean age difference between downwelling and upwelling regions are mainly caused by GHG forcing. The results show that ozone depletion causes an increase in the mean age of air in the Antarctic summer lower stratosphere through two processes: (1) a seasonal delay in the Antarctic polar vortex breakup that inhibits young midlatitude air from mixing with the older air inside the vortex, and (2) enhanced Antarctic downwelling that brings older air from middle and upper stratosphere into the lower stratosphere.

1. Introduction

The strengthening of the stratospheric Brewer-Dobson circulation (BDC) in the past decades is a robust model response to greenhouse gas (GHG) increases and stratospheric ozone depletion (Butchart et al., 2006, 2010). Two diagnostics have been commonly used to study the speed up of the BDC: the increased strength of the stratospheric residual mean circulation (e.g., Butchart & Scaife, 2001; Garcia & Randel, 2008; Hardiman et al., 2013; Li et al., 2008; Lin & Fu, 2013; McLandress & Shepherd, 2009) and the decrease of the stratospheric mean age of air (Austin & Li, 2006; Garcia et al., 2007; Oberländer-Hayn et al., 2015; Oman et al., 2009; Ploeger et al., 2015). The acceleration of the residual circulation is caused by increases in stratospheric Rossby and gravity wave driving (Garcia & Randel, 2008; Shepherd & McLandress, 2011), although Oberländer-Hayn et al. (2016) argued that the acceleration might be interpreted as an upward lift of the stratosphere. Generally an increase of the residual circulation leads to a decrease of the mean age (Li, Waugh, Douglass, Newman, Strahan, et al., 2012), but Neu and Plumb (1999) and Linz et al. (2016) showed that the BDC is directly related to mean age gradient between tropics and extratropics, not the mean age itself. The simulated increase of the residual circulation is supported by indirect observational evidences (e.g., Stolarski et al., 2006; Young et al., 2012). However, the modeled decreasing age trend is not fully consistent with observational and reanalysis studies, particularly in the upper stratosphere (e.g., Diallo et al., 2012; Engel et al., 2009; Ray et al., 2014).

Although the strength of the BDC in a changing climate has been extensively studied (e.g., Butchart, 2014), the relative importance of GHG increases and stratospheric ozone depletion in driving the BDC changes remains uncertain. Separating the impact of GHGs and stratospheric ozone not only improves the attribution of the causes of the past BDC changes but also helps to project future BDC evolution.

The few studies that have attributed BDC changes to GHG and ozone forcing have used different methods to separate these impacts, and the results are not consistent. For instance, the contribution of stratospheric ozone depletion between 1960 and 2000 to the increase of annual-mean tropical upward mass flux at 70 hPa was estimated to be about 60% by Li et al. (2008), about 50% by Oman et al. (2009), and about 16% by McLandress et al. (2010). Examining changes in stratospheric mean age in the past decades, Oman et al. (2009) and Polvani et al. (2018) attributed most of the annual-mean decrease to stratospheric ozone depletion, whereas Oberländer-Hayn et al. (2015) found that GHG and ozone forcing have similar

contributions to mean age changes during austral summer. There is no consensus on the relative importance of GHGs and stratospheric ozone on past changes in the BDC. It is not clear why the results are so different, but the use of different sea surface temperatures (SSTs) could be an important cause due to the large impact of SSTs on the BDC (e.g., Kodama et al., 2007; Oberländer et al., 2013).

The main purpose of this paper is to separate the effects of GHGs and stratospheric ozone on past changes in mean age, including their seasonality, using a coupled atmosphere-ocean version of the Goddard Earth Observing System Chemistry-Climate Model (GEOS CCM). We also investigate the relative roles of GHG increases and stratospheric ozone depletion in driving changes in residual circulation, mean age difference between downwelling and upwelling regions, and diabatic circulation. This work uses a coupled atmosphere-ocean model, ensuring consistency between SSTs and the external forcing. Because SSTs strongly affect the BDC, the use of self-consistent SSTs represents an advance over prior studies (e.g., Oberländer-Hayn et al., 2015; Oman et al., 2009) that used atmospheric models with prescribed SSTs.

A brief introduction of the GEOS CCM and descriptions of experimental design are given in section 2. Results are presented in section 3. Discussion and conclusions are given in section 4.

2. Model and Experimental Design

A coupled atmosphere-ocean version of the GEOS CCM (Li et al., 2016) is used in this study. The atmospheric model is GEOS-5 Fortuna-2.5_p3 (Molod et al., 2012) with 72 layers and a model top at 0.01 hPa. The ocean model is the Modular Ocean Model version 4p1 (Griffies, 2010) with 50 layers. The GEOS CCM used the stratospheric chemistry model of Oman and Douglass (2014). The simulations in this study used horizontal resolution of 2.5° longitude by 2° latitude (atmosphere) and approximately 1° by 1° (ocean). A more detailed description of the GEOS CCM is given in Li et al. (2016), who used the same model and evaluated the simulated climatology with emphasis on the Southern Hemisphere (SH). Overall, the model's performance is comparable to current state-of-the-art climate models.

Three ensembles of transient simulations, for 1960–2010, were run in order to separate the effects of increasing GHGs and decreasing stratospheric ozone on the circulation. Each ensemble includes four members, and the ensemble members differ only in their initial conditions. The first (control) ensemble is forced with the observed changing concentrations of GHGs and ozone depleting substances (ODSs). The other two ensembles include one change: the GHG ensemble uses changing GHGs with fixed 1960 levels of ODSs; the ODS ensemble uses fixed 1960 levels of GHGs and changing ODSs. The use of these three ensembles enables the contributions of GHGs and stratospheric ozone (via ODSs) to changes in the stratospheric mean age to be separated. Unless stated otherwise, monthly mean model outputs are used in this study.

GHG changes affect the BDC both directly through radiative forcing of the atmosphere and indirectly through an impact on the SSTs. The increase of ODSs and subsequent stratospheric ozone loss may also result in a SST response. However, it is found that this indirect effect of stratospheric ozone depletion on the atmosphere via SST changes is small: the ODS ensemble does not exhibit statistically significant zonal mean SST trends in 1960–2010 except in a narrow latitude band near 50°S (not shown). Thus, the zonal mean SST trends in the control ensemble can be attributed predominately to increasing GHGs. This result is consistent with McLandress et al. (2012).

3. Results

3.1. Stratospheric Mean Age of Air

In agreement with previous model studies (e.g., Garcia et al., 2007; Li, Waugh, Douglass, Newman, Strahan, et al., 2012; Oman et al., 2009), the control ensemble simulates a decrease in mean age throughout the stratosphere in the 1960–2010 period (Figure 1a). The decreasing trends in mean age are statistically significant, where the statistical significance is evaluated at the two-tailed 95% confidence interval following Santer et al. (2000). The distributions of the trends in the latitude-pressure section mirror the shape of the climatology, with upward bulging isopleths in the tropics and large vertical gradients in the lower stratosphere. The trends are not hemispherically symmetric in the lower stratosphere, with a stronger decrease in the SH than in the Northern Hemisphere (NH). In the upper stratosphere above about 10 hPa the trends are uniformly distributed in latitude and height.

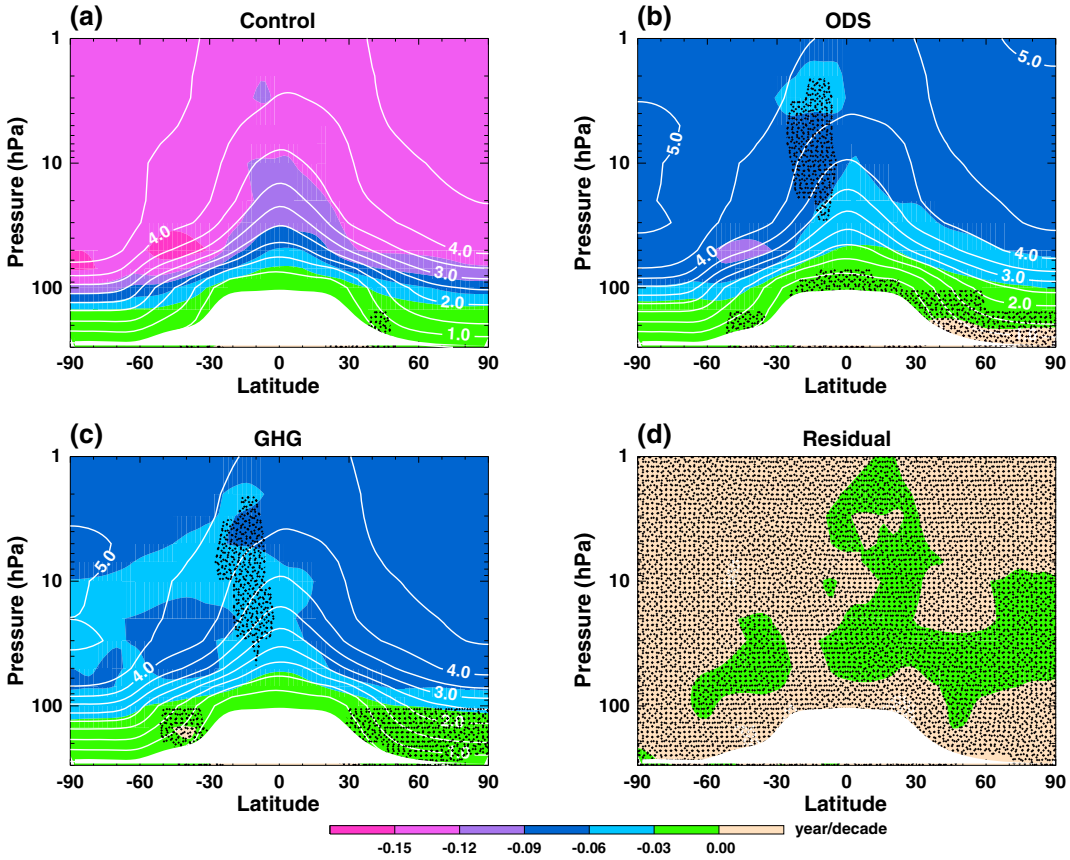

Figure 1. (a–c) Annual mean stratospheric mean age of air climatology (contours) and trends (color shading) in 1960–2010 in the control, ozone depleting substance (ODS), and greenhouse gas (GHG) ensembles. (d) The residual trends of mean age (sum of ODS and GHG minus control) in 1960–2010. Stippling indicates that trends are not statistically significant at the two-tailed 5% level. Contour intervals are 0.5 years in Figures 1a–1c.

The effects of GHG increases and stratospheric ozone depletion on mean age trends can be separated by examining the single forcing ensembles. Figures 1b and 1c show that the ODS and GHG ensembles capture the decreasing trends of stratospheric mean age, with comparable magnitude. The ODS ensemble shows a larger decrease than the GHG ensemble in the SH lower stratosphere. In order to unambiguously attribute the mean age trends to GHGs and ODSs, the linear additivity of the model responses to the two forcings needs to be verified. Here the significance of the residual trends, that is, the sum of the ODS and GHG trends minus the control trends, is used to determine the additivity (McLandress et al., 2011). As can be clearly seen in Figure 1d, the residual trends are not statistically significant, indicating that linear additivity for mean age holds.

The global-averaged mean age trends are used to quantify the relative importance of GHGs and ODSs. Figure 2a shows that GHG increases (red line) and stratospheric ozone depletion (blue line) contribute nearly equally to the annual-mean mean age decrease throughout the stratosphere. The linear additivity of mean age response is clearly seen in Figure 2a as the sum of the GHG and ODS trends (black dashed line) almost overlaps with the control trends (black solid line). The trends in December–February (DJF, Figure 2b) and June–August (JJA, Figure 2c) are similar to the annual-mean trends, indicating weak seasonal variability. Again, GHG and ODS forcings contribute nearly equally to the mean age decrease in DJF and JJA and their contributions are linearly additive.

Although increasing GHGs and decreasing stratospheric ozone have nearly the same effects on the global-averaged mean age trends, their impacts on the latitudinal structure of the trends are different. As shown in Figure 1, ODSs cause a larger mean age decrease than GHGs in the SH lower stratosphere. In order to illustrate this in more detail, the latitudinal distribution of the mean age trends at 70 hPa is compared in Figure 3. ODS-induced trends (blue line) are about 20% stronger than GHG-induced trends (red line) southward of

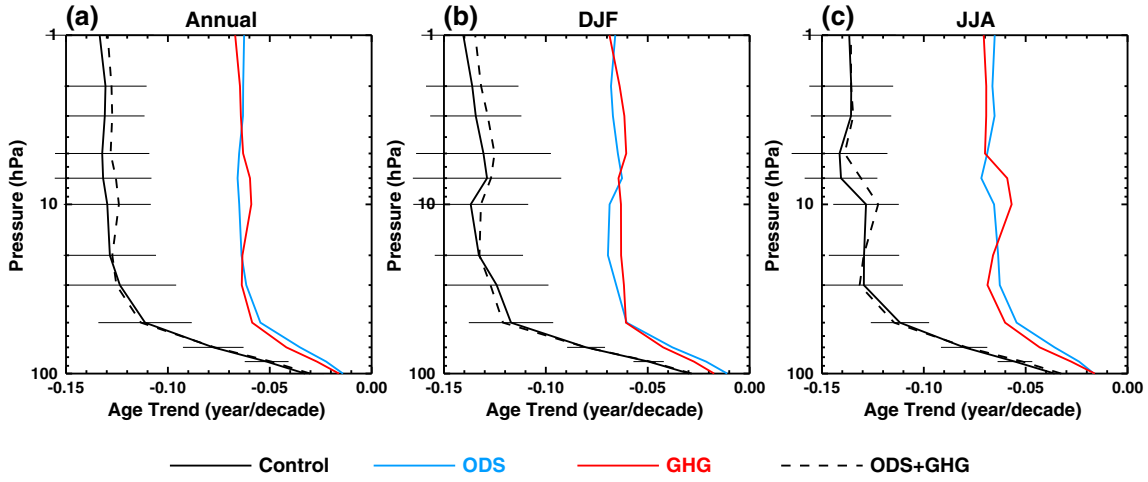

Figure 2. Vertical profiles of global-averaged (a) annual-mean, (b) December–February (DJF), and (c) June–August (JJA) mean age trends in 1960–2010 for the control (black solid line), ozone depleting substance (ODS, blue line), and greenhouse gas (GHG, red line) ensembles. The black dashed lines are the sum of the ODS and GHG trends. The error bars denote 95% confidence interval of the trends in the control ensemble.

30°S but are weaker northward of 30°S. The hemispherically asymmetrical structure of the trends in the control ensemble (black solid line) is mostly caused by stratospheric ozone depletion.

The seasonality of the mean age trends has not been investigated by previous studies. Our results show that the mean age trends have small seasonal variations in most of the stratosphere (Figure 4). Differences between DJF and JJA in the control ensemble are generally small except in the Antarctic lower stratosphere around 100 hPa (Figures 4a and 4d). In this area, the mean age increases in DJF (although the increasing trends are significant only in a small region between 60° and 70°S) and decreases in JJA. This seasonality is solely due to stratospheric ozone depletion (Figures 4b and 4e). The increasing trends in the ODS ensemble are 2 times larger than that in the control ensemble and are mostly significant, but they are partially offset by the decreasing trends in the GHG ensemble (Figure 4c). The processes that cause the mean age increasing trends in the summertime Antarctic lower stratosphere will be discussed in detail in section 3.4.

3.2. Residual Circulation

The Transformed Eulerian Mean (Andrews et al., 1987), or the residual mean meridional circulation, is often used to approximate the BDC. The decrease of the stratospheric mean age is generally associated with the acceleration of the stratospheric residual circulation (Austin & Li, 2006). It should be emphasized that changes in the mean age are affected not only by changes in the residual circulation but also by those in mixing and recirculation (Li, Waugh, Douglass, Newman, Strahan, et al., 2012; Neu & Plumb, 1999; Ploeger et al., 2015). Therefore, the responses of residual circulation and mean age to GHG and ODS forcings could be different.

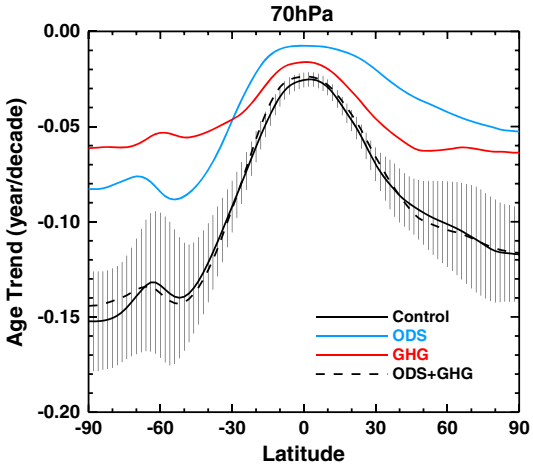

Figure 3. Linear trends of annual-mean stratospheric mean age of air at 70 hPa in 1960–2010 for the control (black solid line), ozone depleting substance (ODS, blue line), and greenhouse gas (GHG, red line) ensembles. The black dashed line is the sum of the ODS and GHG trends. The vertical error bars denote 95% confidence interval of the trends in the control ensemble.

The strength of the residual circulation is defined as the tropical upward mass flux, which equal to the sum of the NH and SH downward mass flux (Rosenlof, 1995). The net downward mass flux in each hemisphere is calculated as

$$2\pi \int_{\varphi_t}^{\text{pole}} \rho a \cos\varphi \overline{w}^* a d\varphi \quad (1)$$

where $\overline{w}^*$ is the residual vertical velocity, ρ is the density, a is the Earth's radius, and φ_t is the turnaround latitude where $\overline{w}^*$ changes from upward to downward. The acceleration of the stratospheric residual circulation, diagnosed in terms of annual-mean tropical upward mass flux, is predominately driven by GHG increases below 10 hPa

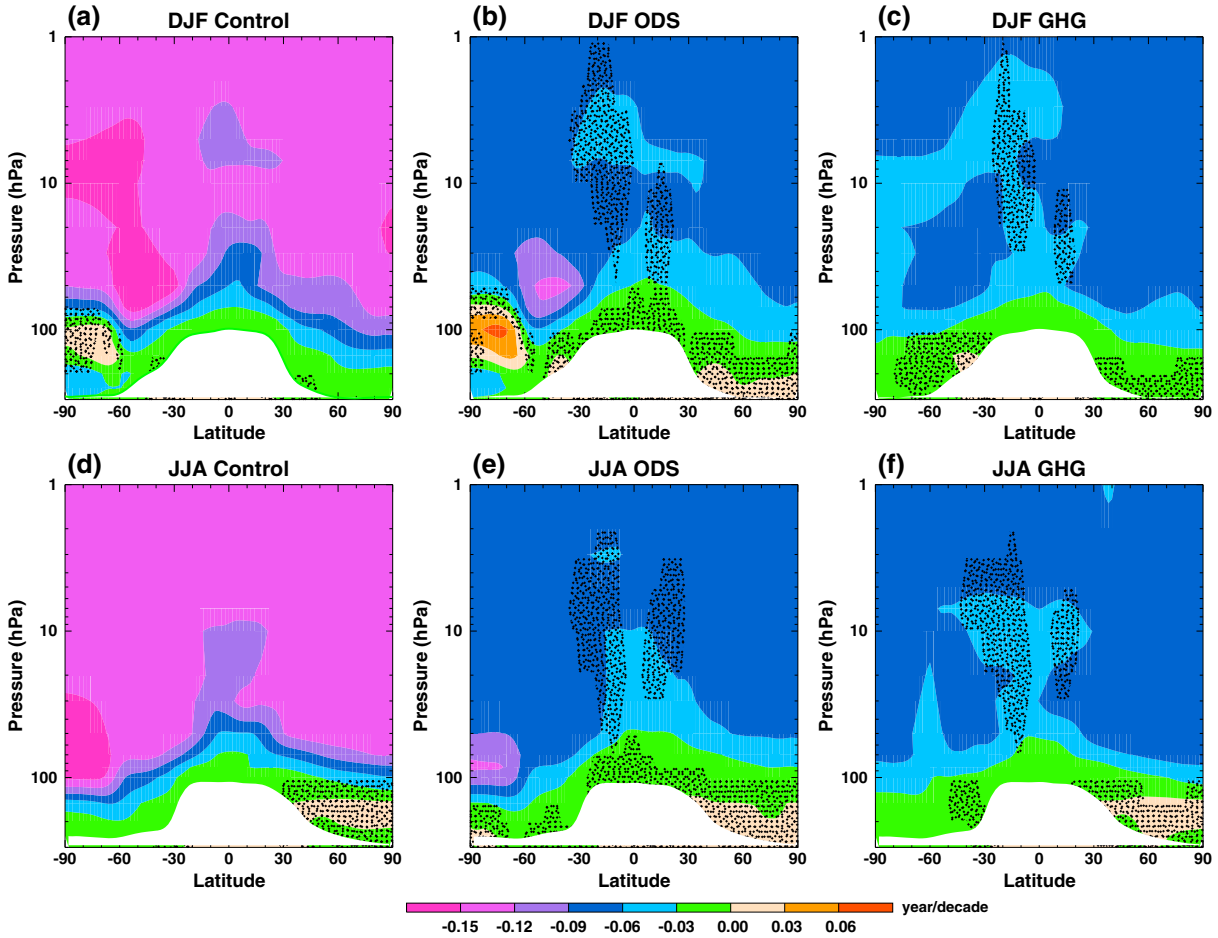

Figure 4. Stratospheric mean age trends in 1960–2010 in December–February (DJF) and June–August (JJA) for (a, d) control, (b, e) ozone depleting substance (ODS), and (c, f) greenhouse gas (GHG) ensembles. Stippling indicates that trends are not statistically significant at the two-tailed 5% level.

(Figure 5a). For example, 64% and 36% of the tropical upwelling trend at 70 hPa is, respectively, caused by GHGs and ODSs. This is in contrast with the nearly equal contributions of GHGs and ODSs to the mean age trends (Figure 2). Another difference between trends in the residual circulation and mean age is that the former has large seasonal variations. The trend at 70 hPa is more than 2 times larger in DJF (2.6×10^8 kg/s/decade) than in JJA (1.1×10^8 kg/s/decade) (Figures 5b and 5c). This seasonality is mainly driven by ODSs, which cause a much stronger trend in DJF (1.4×10^8 kg/s/decade) than in JJA (0.3×10^8 kg/s/decade). Indeed, in DJF at 70 and 50 hPa the ODS ensemble shows slightly larger increasing trends than the GHG ensemble (Figure 5b).

3.3. Mean Age Difference and Diabatic Circulation

It is not surprising that the relative roles between GHGs and ODSs in driving the mean age trends are different from their roles in driving the residual circulation trends, because mean age also depends on mixing. However, isentropic mixing does not affect mean age difference between downwelling and upwelling regions on an isentropic surface in steady state (Linz et al., 2016). Thus, the mean age difference depends only on the mean advection through the isentropic surface, or the diabatic circulation, provided that diabatic diffusion is small. In this section, we investigate the contributions of GHGs and ODSs to changes in mean age difference and diabatic circulation.

In steady state and assuming that diabatic diffusion of age is negligible, Linz et al. (2016) showed that the mass-flux weighted age difference between downwelling and upwelling regions on an isentropic surface (ΔAge) can be calculated as the ratio of the mass above the surface (M) to the upward mass flux through the surface (D).

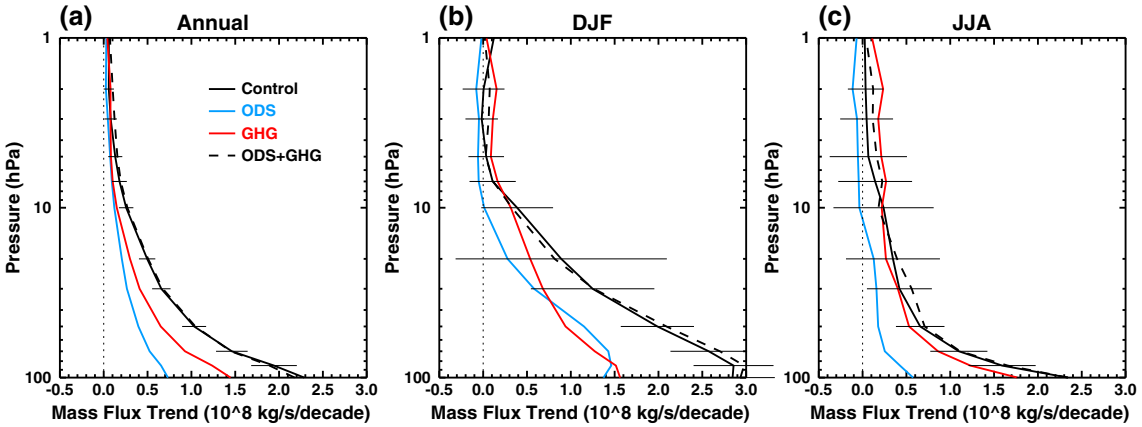

Figure 5. Vertical profiles of (a) annual-mean, (b) December–February (DJF), and (c) June–August (JJA) tropical upward mass flux trends in 1960–2010 for the control (black solid line), ozone depleting substance (ODS, blue line), and greenhouse gas (GHG, red line) ensembles. The black dashed lines are the sum of trends in the ODS and GHG ensembles. The error bars denote 95% confidence interval of the trends in the control ensemble.

$$\Delta\mathrm{Age} = M/D \tag{2}$$

and

$$\Delta\mathrm{Age} = \mathrm{Age}_d - \mathrm{Age}_u = \frac{\int_{\mathrm{up}}\sigma\dot{\theta}\mathrm{Aged}A}{\int_{\mathrm{up}}\sigma\dot{\theta}\mathrm{d}A} - \frac{\int_{\mathrm{down}}\sigma\dot{\theta}\mathrm{Aged}A}{\int_{\mathrm{down}}\sigma\dot{\theta}\mathrm{d}A} \tag{3}$$

$$D = \int_{\mathrm{up}}\sigma\dot{\theta}\mathrm{d}A \tag{4}$$

$$M = \int\sigma\mathrm{d}A\mathrm{d}\theta \tag{5}$$

where $\dot{\theta}$ is the vertical velocity in isentropic coordinates, $\sigma = -\frac{1}{g}\frac{\partial p}{\partial\theta}$ is the density in isentropic coordinates, p is pressure, θ is potential temperature, and A is area on an isentropic surface. The upward mass flux D defines the strength of the diabatic circulation. The vertical velocity $\dot{\theta}$ is calculated from diabatic heating rate. The upwelling and downwelling regions on an isentropic surface are defined where $\dot{\theta}$ is positive or negative, respectively.

The steady state assumption in equation (2) is not valid in 1960–2010 because the diabatic circulation and mean age difference have significant trends in this period (not shown). Therefore, we calculate changes between the 2001–2010 mean and 1960–1969 mean, since the trends within these two decades are not significant and the steady state assumption holds. First, the annual-mean mean age, p, $\dot{\theta}$, and σ are interpolated from pressure surfaces to isentropic surfaces, and the annual-mean ΔAge, M, and D are calculated. Then the decadal mean in 1960–1969 and 2001–2010 and the changes between these two decades are computed. The results are shown in Figure 6. For the 2001–2010 mean in the control ensemble, the mean age difference between the downwelling and upwelling air matches closely with what theory predicts from the ratio of mass to mass flux (Figure 6a). The mean age difference is generally smaller than the ratio of mass to mass flux, which is likely due to neglect of diabatic diffusion in equation (2) (Linz et al., 2016, 2017).

Equation (2) predicts a decrease of the mean age difference with an increase of the diabatic circulation D. Figures 6b and 6c show that the mean age difference and the ratio of mass to mass flux decrease from 1960–1969 to 2001–2010, consistent with theory. GHG forcing is the major driver of both the decrease in mean age difference and ratio of mass to mass flux, accounting, respectively, for about 61% and 67% of their decadal changes in the 400 K–1000 K region. Changes in the mean age difference and the ratio of mass to mass flux have similar vertical structure, but the latter has larger magnitude, which again is likely due to the neglect of diabatic diffusion. The important result here is that the relative roles of GHGs and ODSs in driving changes of the diabatic circulation are similar to their roles in the changes of mean age difference.

3.4. Mean Age Increase in the Summertime Antarctic Lower Stratosphere

The increase of mean age in the Antarctic lower stratosphere during DJF is a unique result from this study. To date, only Oberländer-Hayn et al. (2015) simulated a mean age increase, which occurred in the wintertime

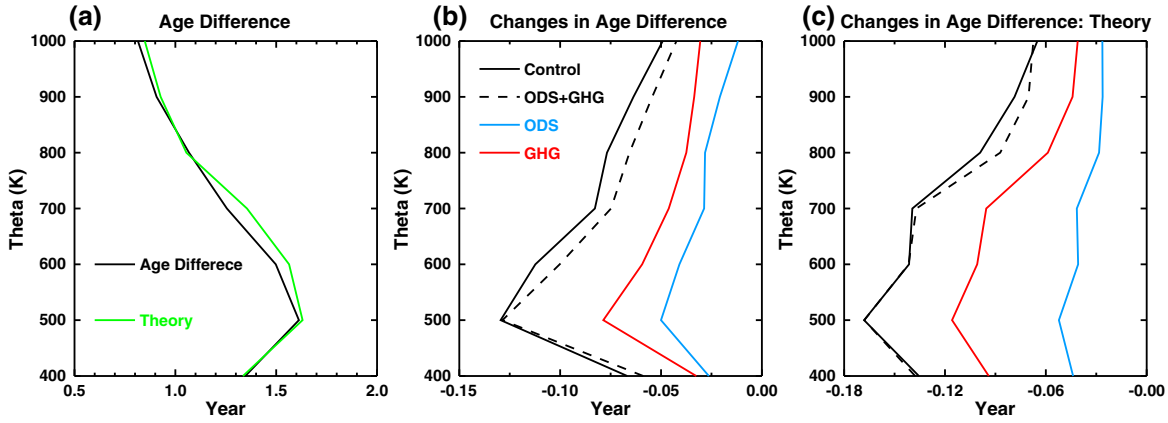

Figure 6. (a) The mean age difference between downwelling and upwelling regions on isentropic surfaces averaged in 2001–2010 (black line) and the ratio of mass above an isentropic surface to mass flux through that surface averaged in 2001–2010 (green line). The results are from the control ensemble. (b) Changes in mean age difference between downwelling and upwelling regions (2001–2010 mean minus 1960–1969 mean) for the control (black solid line), ozone depleting substance (ODS, blue line), and greenhouse gas (GHG, red line) ensembles. The black dashed lines are the sum of the ODS and GHG changes. (c) Same as Figure 6b but for changes in the ratio of mass to mass flux.

Arctic upper stratosphere and lower mesosphere and was caused by a weakening of the residual circulation in that region. However, the mean age increase in our simulations is associated with residual circulation strengthening. Figure 7a shows that the SH residual stream function significantly strengthens during DJF in the control ensemble, which is mostly due to stratospheric ozone depletion, particularly below 10 hPa (Figure 7b). The NH residual circulation also strengthens in DJF, although the trends are weaker and are predominately caused by GHG increases (Figure 7c). The JJA trends are weaker than DJF trends and are attributed mainly to GHG increases (Figures 7d–7f).

We find that the DJF mean age increase is caused by two processes: (1) a delayed breakup of the Antarctic polar vortex, and (2) an enhanced downwelling in the Antarctic lower stratosphere. As we will show below, both processes are caused by stratospheric ozone depletion.

The breakup of the Antarctic polar vortex strongly affects the seasonal evolution of mean age. Figure 8a shows the seasonal cycle of daily mean age in the Antarctic lower stratosphere (averaged south of 64°S at 100 hPa) in the control ensemble. In the pre-ozone hole period (1960–1974, black line), the mean age reaches a maximum value of about 4 years in middle November and then decreases and reaches its minimum value in middle February. This seasonal cycle with oldest air in late spring and youngest air in late summer is determined by the seasonal evolution of stratospheric transport (residual mean circulation and mixing) and Antarctic transport barrier (i.e., the polar vortex) (Konopka et al., 2015; Li, Waugh, Douglass, Newman, Pawson, et al., 2012). During the austral winter and early spring, the strong polar jet suppresses mixing between high and middle latitudes, leading to the accumulation of old air in the Antarctic lower stratosphere brought by the downwelling branch of the residual circulation. As the Antarctic polar vortex breaks up in late spring, mean age starts to decrease by mixing with the midlatitude young air. Thus, the timing of maximum mean age corresponds with the timing of polar vortex/transport barrier breakup.

The seasonal cycle of mean age in the Antarctic lower stratosphere changes significantly between 1960–1974 and 1996–2010. Figure 8a shows that the timing of maximum mean age is delayed from middle November in 1960–1974 to middle December in 1996–2010, indicating a delayed breakup of the Antarctic transport barrier. This delay partly contributes to the mean age increase in 1996–2010 during DJF. The maximum mean age in 1996–2010 is about 0.5 years younger than its counterpart in 1960–1974. But at the time when the Antarctic polar vortex breaks up and the mean age begins to decrease in 1996–2010, this process already takes place for about 1 month in 1960–1974, leading to older mean age in 1996–2010 from middle December to early January.

Comparing the control and single forcing ensembles reveals that the seasonal cycle shift of the mean age is solely driven by stratospheric ozone depletion (Figures 8a–8c). The ODS ensemble shows a similar 3 week

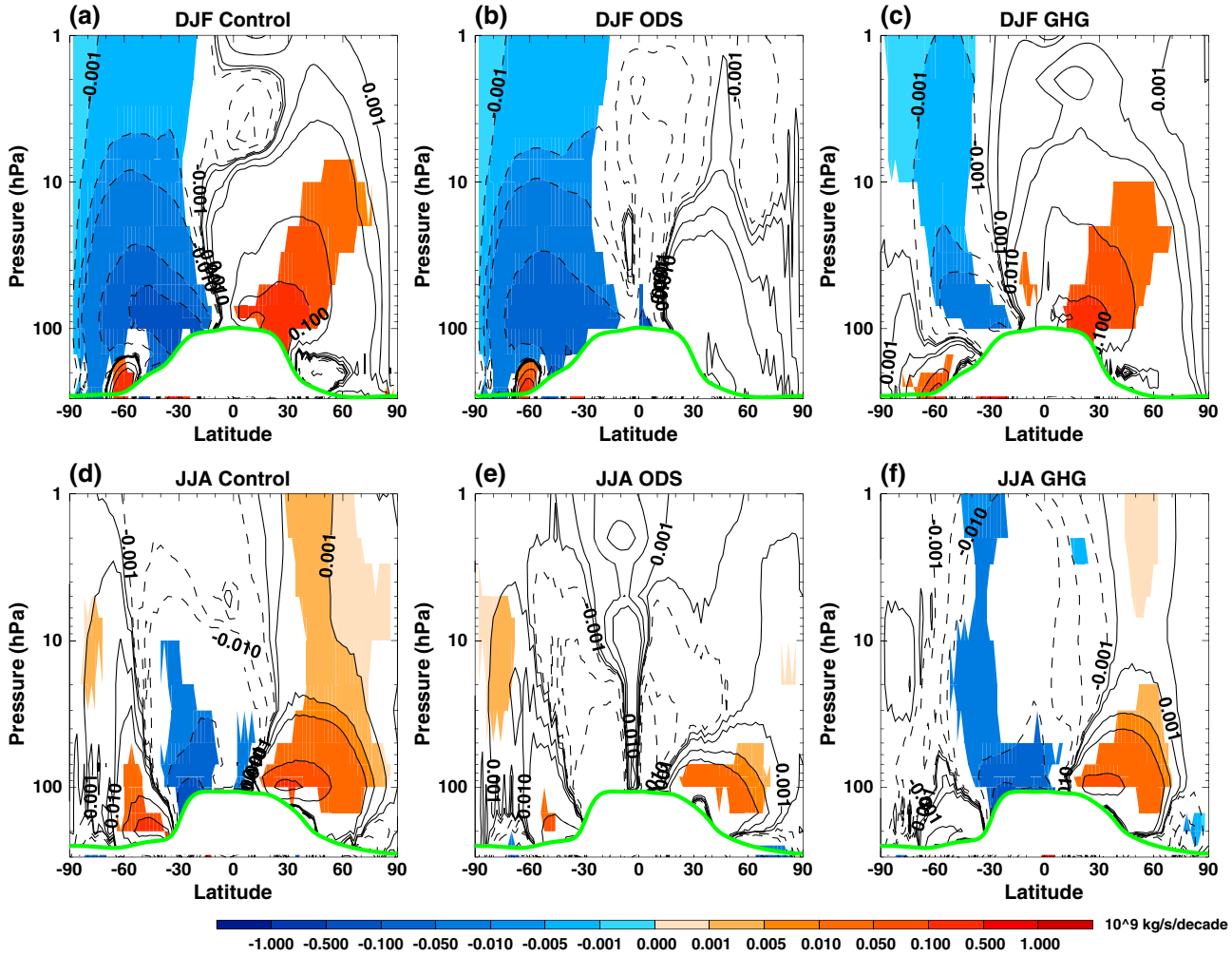

Figure 7. Linear trends of the stratospheric residual mean stream function for the 1960–2010 period in December–February (DJF) and June–August (JJA) for (a, d) control, (b, e) ozone depleting substance (ODS), and (c, f) greenhouse gas (GHG) ensembles. Contour intervals are ±(0, 0.001, 0.005, 0.01, 0.05, 0.1, 0.5, 1) 10^9kg/s/decade. Color shading indicates statistically significant trends. The green line is the climatological tropopause in the control ensemble.

delay in the timing of maximum/minimum mean age as in the control ensemble. The GHG ensemble simulates mean age decrease throughout the year without seasonal cycle change between 1960–1974 and 1996–2010.

The delayed breakup of Antarctic polar vortex is further confirmed by its increased persistence. Figures 8d–8f compare the seasonal evolution of the daily zonal mean zonal wind at 60°S and 100 hPa, used here as a proxy for the polar vortex strength, between 1960–1974 and 1996–2010. We find that in all three ensembles and in both periods, the maximum mean age corresponds to a vortex strength of about 29 m/s, which can be used as a criterion for polar vortex breakup at 100 hPa (e.g., Nash et al., 1996; Waugh et al., 1999). The control ensemble shows stronger westerlies between October and February in 1996–2010 than in 1960–1974 (Figure 8d). The vortex breakup (when the polar jet falls below 29 m/s) is delayed by more than 3 weeks, causing a shift of the mean age seasonal cycle. The strengthening of the polar jet is caused by stratospheric ozone depletion (Figure 8e). GHG increases do not affect the polar jet (Figure 8f).

It has long been recognized that ozone depletion, by cooling the Antarctic lower stratosphere and enhancing the meridional temperature gradient, increases the persistence of Antarctic polar vortex (e.g., Waugh et al., 1999). The delayed Antarctic vortex breakup is not limited to 200–70 hPa where mean age increases but extends throughout the lower to middle stratosphere. Figures 9a and 9b show the seasonal evolution of changes (1996–2010 minus 1960–1974) in daily zonal mean zonal wind at 60°S and daily Antarctic mean

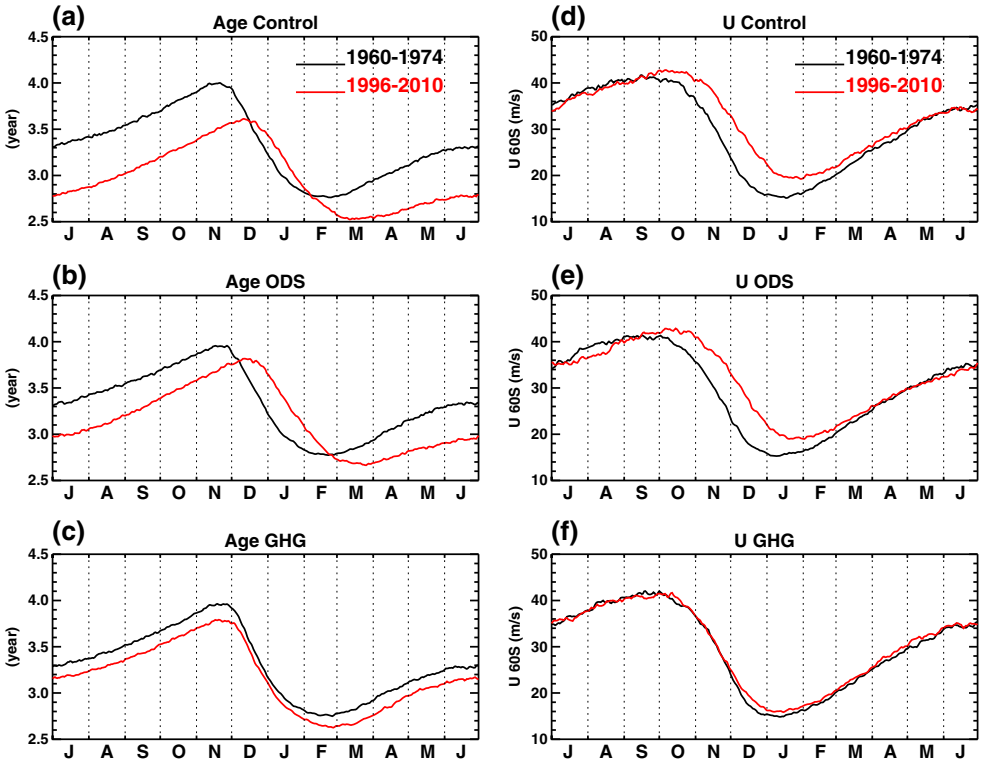

Figure 8. Seasonal evolution of daily Antarctic mean age of air (averaged over 64°–90°S) at 100 hPa in 1960–1974 (black line) and 1996–2010 (red line) for the (a) control, (b) ozone depleting substance (ODS), and (c) greenhouse gas (GHG) ensembles. Same as Figures 8a–8c but for zonal mean zonal wind at 60°S and 100 hPa.

age in the control ensemble, respectively. Between 100 and 10 hPa, the impact of a delayed polar vortex breakup on mean age is clearly seen by reduced mean age decrease from early November to middle December. However, mean age increases only below about 70 hPa. Apparently, other processes also contribute to the summertime Antarctic mean age increase.

We suggest that the strengthening of the Antarctic downwelling, which transports older air from higher levels into the lower stratosphere, plays an important role. Because tropospheric Rossby waves can propagate into the stratosphere only when the mean flow is westerly, the delayed breakup of the Antarctic polar vortex enhances wave driving and increases downwelling in the Antarctic stratosphere (Li et al., 2008; McLandress et al., 2010; Stolarski et al., 2006). Figure 9c shows large increases of the downward residual vertical velocity $\overline{w}^*$ over Antarctica (averaged over 64°–90°S) from late spring to late summer, corresponding with the strengthening of the polar vortex (Figure 9a). However, enhanced downwelling does not always lead to enhanced vertical mean age advection $\left(-\overline{w}^* \frac{\partial \mathrm{Age}}{\partial z}\right)$ because it also depends on the vertical gradient of mean age. Figure 9d shows that a large increase of vertical mean age advection is only found in December and January between about 150 and 70 hPa, where mean age has a strong vertical gradient. The changes in vertical advection can be further decomposed into changes in downwelling and changes in vertical age gradient. It is found that the increase in vertical advection is mainly due to the enhanced downwelling, only at 150 hPa that the increase in vertical gradient makes important contributions (about 50%). The large increase of vertical advection precedes the mean age increase (Figure 9b), supporting our mechanism. The increase in vertical mean age advection in late spring/early summer and the subsequent decrease in late summer in the lower stratosphere are consistent with the changes of mean age seasonal cycle due to the delayed polar vortex breakup, suggesting that enhanced downwelling also contributes to a delayed mean age seasonality. Comparing the vertical advection to the net tendency of mean age, it is found that the increase in vertical advection contributes 25% to the net tendency increase at 100 hPa (not shown), where the largest mean age increase is found. We conclude that the DJF mean age increase is mainly due to a delayed polar vortex breakup, with important contributions from enhanced downwelling.

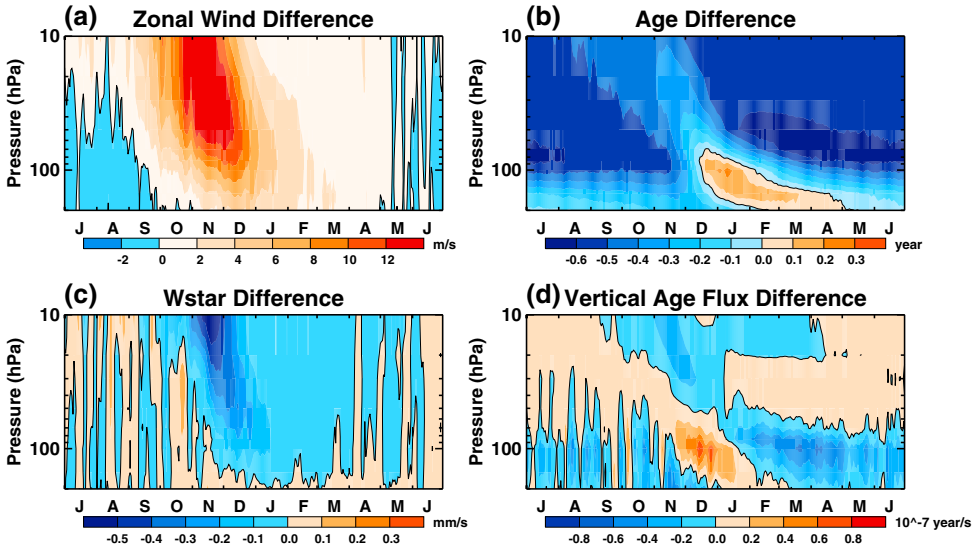

Figure 9. Seasonal evolution of differences (1996–2010 minus 1960–1974) in (a) daily zonal mean zonal wind at 60°S, (b) daily Antarctic mean age of air (averaged over 64°-90°S), (c) daily Antarctic vertical residual velocity (averaged over 64°–90°S), and (d) daily vertical flux of mean age $\left(-\overline{w}^{*}\frac{\partial \mathrm{Age}}{\partial z}\right)$ (averaged over 64°–90°S). Results are from the control ensemble.

Changes in the summertime Antarctic lower stratosphere circulation shown in Figure 9 are predominately driven by stratospheric ozone depletion (not shown). GHG increases do not contribute to the enhanced downwelling and vertical age flux in the Antarctic lower stratosphere (not shown). In summary, Antarctic ozone depletion delays the breakup of the polar vortex and enhances the downward transport of old air into the lower stratosphere, leading to mean age increase.

4. Discussion and Conclusions

The GEOS CCM with a coupled ocean has been used to separate the impact of GHG increases and stratospheric ozone depletion on stratospheric mean age of air, the residual circulation, and the mean age difference between downwelling and upwelling regions in the 1960–2010 period. Three 4-member ensembles of transient simulations were conducted, varying GHGs and ODSs, varying ODSs but fixed 1960 levels of GHGs, and varying GHGs but fixed 1960 levels of ODSs. The relative roles of GHGs and ODSs in driving past trends in the BDC were quantified by comparing these ensembles.

The responses of the stratospheric mean age of air to GHG and ODS forcing are linearly additive in our simulations, meaning that trends in the mean age can be unambiguously attributed to GHGs and ODSs. The results show that GHGs and ODSs contribute nearly equally to the simulated decrease of global-averaged mean age in 1960–2010. However, they have different effects on the latitudinal structure of the mean age trends: GHGs cause a hemispherically uniform mean age decrease, while ODSs induce a stronger mean age decrease in the SH than in the NH. The impact of GHG increases and stratospheric ozone depletion on mean age is seasonally uniform in most of the stratosphere. The exception is in the Antarctic lower stratosphere, where ozone depletion causes large seasonal variations with a mean age increase in DJF and a decrease in JJA.

The relative roles of GHGs and ODSs in driving the residual circulation trends are different from their roles in mean age trends. Stratospheric ozone depletion only accounts for about one third of the annual-mean tropical upward mass flux trend at 70 hPa. In comparison, it accounts for about half of the annual- and global-mean mean age trend. Residual circulation trends due to ozone depletion have large seasonal variations, with a much stronger increase in DJF than in JJA, which is not found in the mean age trends. Our results imply that the projected stratospheric ozone recovery in the 21st century would have a larger impact on future mean age evolution than on future residual circulation changes. Thus, it would be easier to detect a future ozone-recovery signature from a slowdown of decreasing trend of mean age than it would be using changes in the trend of the residual circulation.

Although the qualitative relationship between the stratospheric mean circulation and mean age is well known, quantitatively, it is the mean age difference between downwelling and upwelling regions, not the mean age itself, that is directly related to the mean overturning circulation (Linz et al., 2016). Our calculations show that the decrease in the mean age difference is consistent with what theory predicts from the increase in the tropical upward mass flux. GHG forcing is a major driver of the decrease in the mean age difference, consistent with its role in the acceleration of the BDC. These results indicate that the mean age difference between downwelling and upwelling regions should be an important metric to study changes in the BDC.

Long-term observations of mean age are scarce, and they do not show significant mean age decreases throughout the stratosphere, contrary to model results (e.g., Engel et al., 2009; Ray et al., 2010, 2014). The simulated mean age increase in the Antarctic lower stratosphere during DJF thus provides novel insights into the mechanisms at work. The increase in mean age is not caused by weakening of the residual circulation, as might be expected intuitively, but is due to the combined effects of a delayed breakup of Antarctic transport barrier and enhanced downwelling in the Antarctic lower stratosphere. Both processes are mostly attributed to ozone depletion. Stratospheric ozone depletion cools the Antarctic lower stratosphere in spring and increases the persistence of the polar vortex, leading to (1) a delayed breakup of the polar vortex, which delays the mixing of younger air from middle latitude with the older Antarctic air, and (2) enhanced Antarctic downwelling that transports more old air from higher levels into the lower stratosphere. These two processes cause the mean age to increase in the summertime Antarctic lower stratosphere, with the delayed Antarctic polar vortex breakup playing a more important role. This mechanism cannot explain the reported mean age increase in the NH extratropics (Engel et al., 2009) or in the polar upper stratosphere (Stiller et al., 2012).

Our finding demonstrates a special case that an enhanced BDC leads to an increase of mean age, contrary to the conventional view. This discrepancy can be explained in the framework of age spectrum, in which changes in the mean age are determined by changes in the relative importance of young air with fast pathways and old air with slow pathways in the age spectrum (Li, Waugh, Douglass, Newman, Strahan, et al., 2012). In the case of Antarctic summertime lower stratosphere, the major fast pathway is mixing with midlatitude lower stratosphere and the major slow pathway is descent from Antarctic upper stratosphere through the deep branch of the BDC. An enhanced Antarctic downwelling causes an increase in the percentages of old air, which contributes to the increase of mean age. A delayed breakup of the Antarctic transport barrier reduces the percentages of young air. Together, these two processes lead to an increase of mean age.

Our proposed mechanism is partly supported by observations that show a delay in Antarctic polar vortex breakup and increases in the summertime Antarctic downward transport (Stolarski et al., 2006; Waugh et al., 1999). However, the Antarctic polar vortex in GEOS CCM is too persistent (not shown), a common bias in almost all the CCMs (Eyring et al., 2006). This bias may amplify the dynamical response to stratospheric ozone depletion (Fogt et al., 2009; Lin et al., 2017). Therefore, GEOS CCM might overestimate the increase of mean age in the summertime Antarctic lower stratosphere.

The results of this study need to be interpreted in the context of those from a related study of Garfinkel et al. (2017), who showed that the simulated trends of the BDC depend on the duration of the period, and the start and end dates used for calculation. While some of our results agree with the small number of previous studies in this topic, there are some substantial differences. For example, Oman et al. (2009) found that stratospheric ozone depletion is much more important than GHG increases in causing the mean age decrease. Oberländer-Hayn et al. (2015) found that the mean age responses to GHG and ODS forcings are not linearly additive in their simulations. These different results could be caused by differences in models or methods. The use of a coupled atmosphere-ocean model (this study) versus prescribed SSTs (Oberländer-Hayn et al., 2015; Oman et al., 2009) could have an impact on model results. In order to better understand the roles of the GHGs and stratospheric ozone in driving past changes and future evolution of the BDC, single forcing experiments under the coupled atmosphere-ocean-chemistry model framework from more modeling groups are needed.

Acknowledgments
This work was supported by NASA's Modeling, Analysis and Prediction Program (MAP) under grants NNX13AN98G and NNX13AM24G. NASA Center for Climate Simulation (NCCS) provided computational resources for this work. The simulations used in this study are stored in the data-storage facilities at NCCS and are fully available upon a request to F. L. (feng.li@nasa.gov).

References

Andrews, D. G., Holton, J. R., & Leovy, C. B. (1987). *Middle atmosphere dynamics*, *International geophysical series* (Vol. 40, p. 489). Orlando, FL: Academic Press.

Austin, J., & Li, F. (2006). On the relationship between the strength of the Brewer-Dobson circulation and the age of stratospheric air. *Geophysical Research Letters*, *33*, L17807. https://doi.org/10.1029/2006GL026867

Butchart, N. (2014). The Brewer-Dobson circulation. *Reviews of Geophysics*, *52*, 157–184. https://doi.org/10.1002/2013RG000448

Butchart, N., Cionni, I., Eyring, V., Shepherd, T. G., Waugh, D. W., Akiyoshi, H., et al. (2010). Chemistry-climate model simulations of twenty-first century stratospheric climate and circulation change. *Journal of Climate*, *23*(20), 5349–5374. https://doi.org/10.1175/2010JCLI3404.1

Butchart, N., & Scaife, A. A. (2001). Removal of chlorofluorocarbons by increased mass exchange between the stratosphere and troposphere in a changing climate. *Nature*, *410*(6830), 799–802. https://doi.org/10.1038/35071047

Butchart, N., Scaife, A. A., Bourqui, M., de Grandpré, J., Hare, S. H. E., Kettleborough, J., et al. (2006). Simulations of anthropogenic change in the strength of the Brewer–Dobson circulation. *Climate Dynamics*, *27*(7-8), 727–741. https://doi.org/10.1007/s00382-006-0162-4

Diallo, M., Legras, B., & Chedin, A. (2012). Age of stratospheric air in the ERA-Interim. *Atmospheric Chemistry and Physics*, *12*(24), 12,133–12,154. https://doi.org/10.5194/acp-12-12133-2012

Engel, A., Möbius, T., Bönisch, H., Schmidt, U., Heinz, R., Levin, I., et al. (2009). Age of stratospheric air unchanged within uncertainties over the past 30 years. *Nature Geoscience*, *2*(1), 28–31. https://doi.org/10.1038/ngeo388

Eyring, V., Butchart, N., Waugh, D. W., Akiyoshi, H., Austin, J., Bekki, S., et al. (2006). Assessment of temperature, trace species, and ozone in chemistry-climate model simulations of the recent past. *Journal of Geophysical Research*, *111*, D22308. https://doi.org/10.1029/2006JD007327

Fogt, R. L., Perlwitz, J., Pawson, S., & Olsen, M. A. (2009). Intra-annual relationships between polar ozone and the SAM. *Geophysical Research Letters*, *36*, L04707. https://doi.org/10.1029/2008GL036627

Garcia, R. R., Marsh, D. R., Kinnison, D. E., Boville, B. A., & Sassi, F. (2007). Simulation of secular trends in the middle atmosphere, 1950–2003. *Journal of Geophysical Research*, *112*, D09301. https://doi.org/10.1029/2006JD007485

Garcia, R. R., & Randel, W. (2008). Acceleration of the Brewer–Dobson circulation due to increases in greenhouse gases. *Journal of the Atmospheric Sciences*, *65*(8), 2731–2739. https://doi.org/10.1175/2008JAS2712.1

Garfinkel, C. I., Aquila, V., Waugh, D. W., & Oman, L. D. (2017). Time-varying changes in the simulated structure of the Brewer-Dobson circulation. *Atmospheric Chemistry and Physics*, *17*(2), 1313–1327. https://doi.org/10.5194/acp-17-1313-2017

Griffies, S. M. (2010). Elements of MOM4p1. GFDL Ocean Group Tech. Rep. 6 (444 pp.). Retrieved from https://gfdl.noaa.gov/cms-filesystem-action/model_development/ocean/momguide4p1.pdf

Hardiman, S. C., Butchart, N., & Calvo, N. (2013). The morphology of the Brewer-Dobson circulation and its response to climate change in CMIP5 simulations. *Quarterly Journal of the Royal Meteorological Society*, *140*(683), 1958–1965. https://doi.org/10.1002/qj.2258

Kodama, C., Iwasaki, T., Shibata, K., & Yukimoto, S. (2007). Changes in the stratospheric mean meridional circulation due to increased CO_2: Radiation- and sea surface temperature-induced effects. *Journal of Geophysical Research*, *112*, D16103. https://doi.org/10.1029/2006JD008219

Konopka, P., Ploeger, F., Tao, M., Birner, T., & Riese, M. (2015). Hemispheric asymmetries and seasonality of mean age of air in the lower stratosphere: Deep versus shallow branch of the Brewer-Dobson circulation. *Journal of Geophysical Research: Atmospheres*, *120*, 2053–2066. https://doi.org/10.1002/2014JD022429

Li, F., Austin, J., & Wilson, J. (2008). The strength of the Brewer–Dobson circulation in a changing climate: Coupled chemistry–climate model simulations. *Journal of Climate*, *21*(1), 40–57. https://doi.org/10.1175/2007JCLI1663.1

Li, F., Vikhliaev, Y. V., Newman, P. A., Pawson, S., Perlwitz, J., Waugh, D. W., & Douglass, A. R. (2016). Impacts of interactive stratospheric chemistry on Antarctic and Southern Ocean climate change in the Goddard Earth Observing System, version 5 (GEOS-5). *Journal of Climate*, *29*(9), 3199–3218. https://doi.org/10.1175/JCLI-D-15-0572.1

Li, F., Waugh, D., Douglass, A. R., Newman, P. A., Pawson, S., Stolarski, R. S., et al. (2012). Seasonal variations of stratospheric age spectra in GEOSCCM. *Journal of Geophysical Research*, *117*, D05134. https://doi.org/10.1029/2011JD016877

Li, F., Waugh, D. W., Douglass, A. R., Newman, P. A., Strahan, S. E., Ma, J., et al. (2012). Long-term changes in stratospheric age spectra in the 21st century in the Goddard Earth Observing System Chemistry-Climate Model (GEOSCCM). *Journal of Geophysical Research*, *117*, D20119. https://doi.org/10.1029/2012JD017905

Lin, P., & Fu, Q. (2013). Changes in various branches of the Brewer–Dobson circulation from an ensemble of chemistry climate models. *Journal of Geophysical Research: Atmospheres*, *118*, 73–84. https://doi.org/10.1029/2012JD018813

Lin, P., Paynter, D., Polvani, L., Correa, G. J. P., Ming, Y., & Ramaswamy, V. (2017). Dependence of model-simulated response to ozone depletion on stratospheric polar vortex climatology. *Geophysical Research Letters*, *44*, 6391–6398. https://doi.org/10.1002/2017GL073862

Linz, M., Plumb, R. A., Gerber, E. P., Haenel, F. J., Stiller, G., Kinnison, D. E., et al. (2017). The strength of the meridional overturning circulation of the stratosphere. *Nature Geoscience*, *10*(9), 663–667. https://doi.org/10.1038/NGEO3013

Linz, M., Plumb, R. A., Gerber, E. P., & Sheshadri, A. (2016). The relationship between age of air and the diabatic circulation of the stratosphere. *Journal of the Atmospheric Sciences*, *73*(11), 4507–4518. https://doi.org/10.1175/JAS-D-16-0125.1

McLandress, C., Jonsson, A. I., Plummer, D. A., Reader, M. C., Scinocca, J. F., & Shepherd, T. G. (2010). Separating the dynamical effects of climate change and ozone depletion. Part I: Southern Hemisphere stratosphere. *Journal of Climate*, *23*(18), 5002–5020. https://doi.org/10.1175/2010JCLI3586.1

McLandress, C., Perlwitz, J., & Shepherd, T. G. (2012). Comment on "Tropospheric temperature response to stratospheric ozone recovery in the 21st century" by Hu et al. (2011). *Atmospheric Chemistry and Physics*, *12*(5), 2533–2540. https://doi.org/10.5194/acp-12-2533-2012

McLandress, C., & Shepherd, T. G. (2009). Simulated anthropogenic changes in the Brewer-Dobson circulation, including its extension to high latitudes. *Journal of Climate*, *22*(6), 1516–1540. https://doi.org/10.1175/2008JCLI2679.1

McLandress, C., Shepherd, T. G., Scinocca, J. F., Plummer, D. A., Sigmond, M., Jonsson, A. I., & Reader, M. C. (2011). Separating the dynamical effects of climate change and ozone depletion. Part II: Southern Hemisphere troposphere. *Journal of Climate*, *24*(6), 1850–1868. https://doi.org/10.1175/2010JCLI3958.1

Molod, A., Takacs, L., Suarez, M., Bacmeister, J., Song, I. S., & Eichmann, A. (2012). The GEOS-5 atmospheric general circulation model: Mean climate and development from MERRA to Fortuna. Technical Report Series on Global Modeling and Data Assimilation, Rep. 28 (115 pp.). Retrieved from http://gmao.gsfc.nasa.gov/pubs/docs/Molod484.pdf

Nash, E. R., Newman, P. A., Rosenfield, J. E., & Schoeberl, M. R. (1996). An objective determination of the polar vortex using Ertel's potential vorticity. *Journal of Geophysical Research*, *101*, 9471–9478.

Neu, J. L., & Plumb, R. A. (1999). Age of air in a "leaky pipe" model of stratospheric transport. *Journal of Geophysical Research*, *104*, 19,243–19,255. https://doi.org/10.1029/1999JD900251

Oberländer, S., Langematz, U., & Meul, S. (2013). Unraveling impact factors for future changes in the Brewer-Dobson circulation. *Journal of Geophysical Research: Atmospheres*, *118*, 10,296–10,312. https://doi.org/10.1002/jgrd.50775

Oberländer-Hayn, S., Gerber, E. P., Abalichin, J., Akiyoshi, H., Kerschbaumer, A., Kubin, A., et al. (2016). Is the Brewer-Dobson circulation increasing or moving upward? *Geophysical Research Letters*, *43*, 1772–1779. https://doi.org/10.1002/2015GL067545

Oberländer-Hayn, S., Meul, S., Langematz, U., Abalichin, J., & Haenel, F. (2015). A chemistry-climate model study of past changes in the Brewer-Dobson circulation. *Journal of Geophysical Research: Atmospheres*, *120*, 6742–6757. https://doi.org/10.1002/2014JD022843

Oman, L., Waugh, D. W., Pawson, S., Stolarski, R. S., & Newman, P. A. (2009). On the influence of anthropogenic forcings on changes in the stratospheric mean age. *Journal of Geophysical Research*, *114*, D03105. https://doi.org/10.1029/2008JD010378

Oman, L. D., & Douglass, A. R. (2014). Improvements in total column ozone in GEOSCCM and comparisons with a new ozone-depleting substances scenario. *Journal of Geophysical Research: Atmospheres*, *119*, 5613–5624. https://doi.org/10.1002/2014JD021590

Ploeger, F., Abalos, M., Birner, T., Konopka, P., Legras, B., Müller, R., & Riese, M. (2015). Quantifying the effects of mixing and residual circulation on trends of stratospheric mean age of air. *Geophysical Research Letters*, *42*, 2047–2054. https://doi.org/10.1002/2014GL062927

Polvani, L. M., Abalos, M., Garcia, R., Kinnison, D., & Randel, W. J. (2018). Significant weakening of Brewer-Dobson circulation trends over the 21st century as a consequence of Montreal Protocol. *Geophysical Research Letters*, *45*, 401–409. https://doi.org/10.1002/2017GL075345

Ray, E. A., Moore, F. L., Rosenlof, K. H., Davis, S. M., Boenisch, H., Morgenstern, O., et al. (2010). Evidence for changes in stratospheric transport and mixing over the past three decades based on multiple data sets and tropical leaky pipe analysis. *Journal of Geophysical Research*, *115*, D21304. https://doi.org/10.1029/2010JD014206

Ray, E. A., Moore, F. L., Rosenlof, K. H., Davis, S. M., Sweeney, C., Tans, P., et al. (2014). Improving stratospheric transport trend analysis based on SF_6 and CO_2 measurements. *Journal of Geophysical Research: Atmospheres*, *119*, 14,110–14,128. https://doi.org/10.1002/2014JD021802

Rosenlof, K. H. (1995). Seasonal cycle of the residual mean meridional circulation in the stratosphere. *Journal of Geophysical Research*, *100*, 5173–5191.

Santer, B., Wigley, T., Boyle, J., Gaffen, D., Hnilo, J., Nychka, D., et al. (2000). Statistical significance of trends and trend differences in layer-average atmospheric temperature time series. *Journal of Geophysical Research*, *105*, 7337–7356. https://doi.org/10.1029/1999JD901105

Shepherd, T. G., & McLandress, C. (2011). A robust mechanism for strengthening of the Brewer-Dobson circulation in response to climate change: Critical-layer control of subtropical wave breaking. *Journal of the Atmospheric Sciences*, *68*(4), 784–797. https://doi.org/10.1175/2010JAS3608.1

Stiller, G. P., von Clarmann, T., Haenel, F., Funke, B., Glatthor, N., Grabowski, U., et al. (2012). Observed temporal evolution of global mean age of stratospheric air for the 2002 to 2010 period. *Atmospheric Chemistry and Physics*, *12*(7), 3311–3331. https://doi.org/10.5194/acp-12-3311-2012

Stolarski, R. S., Douglass, A. R., Gupta, M., Newman, P. A., Pawson, S., Schoeberl, M. R., & Nielsen, J. E. (2006). An ozone increase in the Antarctic summer stratosphere: A dynamical response to the ozone hole. *Geophysical Research Letters*, *33*, L21805. https://doi.org/10.1029/2006GL026820

Waugh, D. W., Randel, W. J., Pawson, S., Newman, P. A., & Nash, E. R. (1999). Persistence of the lower stratospheric polar vortices. *Journal of Geophysical Research*, *104*, 27,191–27,201. https://doi.org/10.1029/1999JD900795

Young, P. J., Rosenlof, K. H., Solomon, S., Sherwood, S. C., Fu, Q., & Lamarque, J.-F. (2012). Changes in stratospheric temperatures and their implications for changes in the Brewer-Dobson circulation, 1979–2005. *Journal of Climate*, *25*(5), 1759–1772. https://doi.org/10.1175/2011JCLI4048.1